

## Low-frequency radio observations of Galactic X-ray binary systems

---

**James Miller-Jones<sup>\*,abc</sup>, Anna Kapińska,<sup>a</sup> Katherine Blundell,<sup>d</sup> Ben Stappers,<sup>ea</sup>  
Robert Braun,<sup>f</sup> and the LOFAR Transients Key Project collaboration<sup>g</sup>**

<sup>a</sup>*Astronomical Institute 'Anton Pannekoek', University of Amsterdam, Kruislaan 403, 1098 SJ, Amsterdam, the Netherlands*

<sup>b</sup>*Jansky Fellow, National Radio Astronomy Observatory*

<sup>c</sup>*National Radio Astronomy Observatory, 520 Edgemont Road, Charlottesville, VA 22903, USA*

<sup>d</sup>*Astrophysics, Denys Wilkinson Building, Keble Road, Oxford, OX1 3RH, UK*

<sup>e</sup>*Stichting ASTRON, Postbus 2, 7990 AA Dwingeloo, The Netherlands.*

<sup>f</sup>*Australia Telescope National Facility, CSIRO, PO Box 76, Epping NSW 1710, Australia.*

<sup>g</sup>[http://www.astro.uva.nl/lofar\\_transients/lofar\\_team.html](http://www.astro.uva.nl/lofar_transients/lofar_team.html)

*E-mail: jmiller@nrao.edu, akapinsk@science.uva.nl,*

*kmb@astro.ox.ac.uk, bws@science.uva.nl, robert.braun@csiro.au*

With the advent of facilities enabling wide-field monitoring of the dynamic radio sky, new areas of parameter space will be opened up for exploration. Such monitoring will be done primarily at low frequencies, in order to maximise the available field of view. One class of radio sources known to be highly variable at GHz frequencies are the so-called 'microquasars', X-ray binaries with relativistic jets. To date however, their low-frequency behaviour has not been well constrained by observations. I will present some of the first attempts to measure their low-frequency properties, showing wide-field images made from data taken with the 74-MHz system on the Very Large Array (VLA) and also the Low Frequency Front Ends (LFFEs), the new suite of low-frequency (117–175 MHz) receivers on the Westerbork Synthesis Radio Telescope (WSRT). I will show results including the low-frequency spectra of the three X-ray binaries SS 433, GRS 1915+105 and Cygnus X-3, a low-frequency study of the W 50 nebula surrounding SS 433, a search for synchrotron lobes inflated by the jets of GRS 1915+105, and the evolution of the May 2006 outburst of Cygnus X-3 at MHz frequencies.

*Bursts, Pulses and Flickering: Wide-field monitoring of the dynamic radio sky*

*June 12-15 2007*

*Kerastari, Tripolis, Greece*

---

\*Speaker.

## 1. Introduction

Technology advances in recent years have provided the hardware and processing power to enable low-frequency observations with wide bandwidths to be correlated, calibrated and imaged over very large fields of view. This enables the monitoring of large areas of the sky in the radio band, providing for the first time a radio all-sky monitor to search for transients at MHz frequencies. In addition, instruments observing at low frequencies are sensitive to coherent events which cannot be seen at higher radio frequencies. For synchrotron-emitting jet-like sources, low frequency observations allow us to probe the shape of the low energy electron distribution to determine whether there is a cutoff, and to accurately constrain the energetics of the jets from unbeamed radio fluxes or calorimetry of jet-blown lobes (e.g. [6]). Monitoring a large area of the radio sky over a long period of time will also allow the creation of a detailed census of transient sources, enabling us to better determine their duty cycles.

In these proceedings, I will present low-frequency radio observations of three X-ray binary systems known to produce relativistic jets; SS 433, GRS 1915+105, and Cygnus X-3. These were selected as persistently bright radio emitters at GHz frequencies, and therefore suitable candidates for a low-frequency radio investigation as part of a preliminary study for the LOFAR Transients Key Science Project [5].

## 2. Observations and data analysis

### 2.1 VLA observations

We observed SS 433 in all four VLA configurations between January and October 2001. The data were taken in the '4P' mode, observing simultaneously at 74 MHz in one of the two independent frequency bands (IF pairs) and at 330 MHz in the other. Data were taken in spectral line mode, in order to enable RFI excision and prevent bandwidth smearing far from the image centre. Data reduction was carried out using AIPS. Cygnus A was used at both frequencies for bandpass calibration and also for determining the antenna gains and phases with a publicly-available model<sup>1</sup>. The data were then averaged in frequency, and several imaging and phase-only self-calibration cycles were performed on the datasets from the individual array configurations. We attempted to mitigate the detrimental effects of ionospheric phase gradients for the A and B configuration data by using a form of ionospheric modelling whereby the positional shifts of the known sources from the NRAO VLA Sky Survey (NVSS) across the field of view were fitted with a second-order Zernike polynomial for each time interval [2]. This algorithm enabled us to calibrate the 74-MHz B-configuration observations, but the ionospheric effects were too great to recover anything from the A-configuration data.

The large size of the primary beam ( $\sim 11.9^\circ$  FWHM at 74 MHz) meant that we detected bright sources far from the pointing centre which had to be properly deconvolved to prevent their sidelobes from influencing the quality of the final images in the region of interest near the centre of the field. In order to account for the non-coplanar nature of the array when imaging, the full primary beam (and beyond) was subdivided into a large number of facets, each with a different

---

<sup>1</sup><http://rsd-www.nrl.navy.mil/7210/7213/LWA/tutorial/>

tangent plane and small enough to obey the small-field approximation and thus to be imaged in two dimensions. Finally, the data sets from the different array configurations were then concatenated and a deconvolution and phase-only self-calibration were performed on the whole data set before the final image was made.

## 2.2 WSRT observations

In 2005 July, we observed our three target X-ray binaries for 12 hours each with the new Low Frequency Front End (LFFE) receivers on the Westerbork Synthesis Radio Telescope (WSRT). These receivers provide eight 2.5-MHz observing bands (IFs) between 117 and 175 MHz. Observations within each band were made with 128 channels, 10-s integrations, 4 polarisations and 2-bit sampling. In all cases, the array was in its  $2 \times 96$  m configuration. The low declinations of SS 433 and GRS 1915+105 meant both that much of the short baseline  $uv$ -coverage had to be excised for these sources due to shadowing concerns, and that the restoring beamsize was severely extended in the N-S direction, degrading the resolution. The primary beam size was of order  $6\text{--}8^\circ$  on a side, such that very large areas of sky had once again to be imaged and deconvolved. The observations were all carried out at night, when the radio frequency interference (RFI) situation was least bad. Each 12-h run in the LFFE band was followed by a 12-h run the next night in the 92-cm band, which comprised eight separate IFs in the frequency range 320–380 MHz. Four further 12-hour observations of Cygnus X-3 were made in the LFFE band only, during the flare of 2006 May, to track the flux density evolution of the source at low-frequencies.

The data were Hanning smoothed before being run through various RFI-rejection algorithms and converted into UVFITS format for further processing with AIPS. System temperature information was used to make an initial calibration of the amplitude gains of the telescope, and any remaining RFI was excised. Bandpass calibration was then performed using one of the calibrator sources 3C 48 and 3C 295, which was then used to set the flux density scale and perform some initial calibration of the phase gains. Following this, an iterative process of imaging and self-calibration was carried out to make the final images, independently self-calibrating on and subtracting (peeling) the brightest sources in each field to account for direction-dependent phase solutions. Since the WSRT is a linear array, the need for facetting during the imaging process was eliminated.

## 3. Results

### 3.1 Persistent X-ray binaries in non-flaring states

SS 433 was clearly detected in both sets of observations (VLA and LFFE). The VLA image is shown in Figure 1. SS 433 is in the centre of the image, surrounded by the W 50 nebula, and the field is dominated by the supernova remnants in the Galactic Plane.

The non-contemporaneous nature of the observing runs prevents us from using all the observations to determine a spectrum down to 74 MHz, although since the 140- and 350-MHz runs were taken on subsequent nights, we were able to construct a spectrum across these two bands. Between 160 and 320 MHz the spectrum is steep, with a spectral index of  $\alpha = -1.3$  ( $S_\nu \propto \nu^\alpha$ ), but inverts to a spectral index of 2.1 at around 330 MHz. This suggests that the observed emission comes from recently-ejected, optically thick components responsible for the inverted spectrum, superposed on

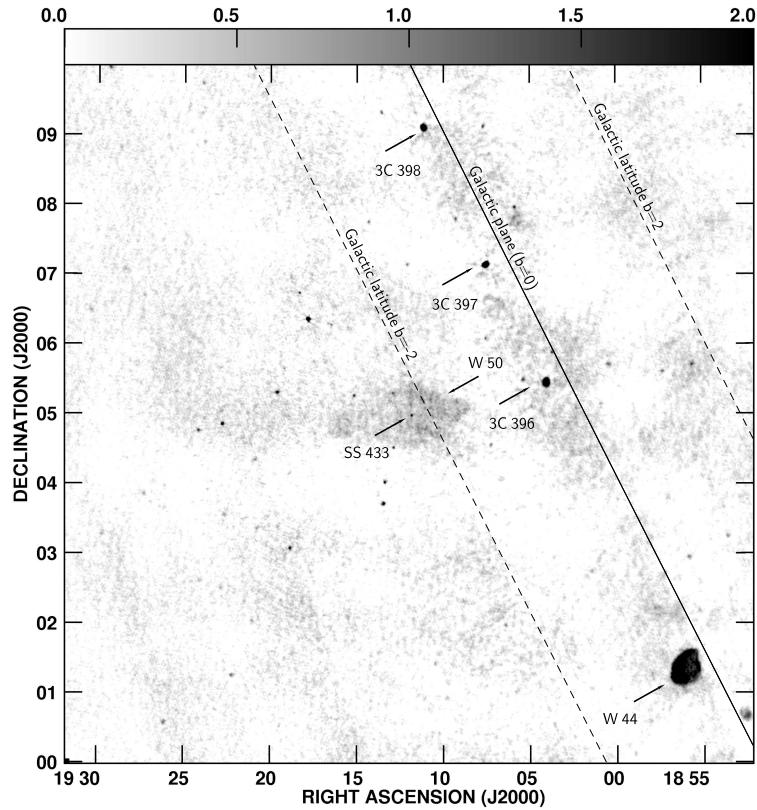


**Figure 1:**  $10^\circ \times 10^\circ$  74-MHz image made using B, C and D configuration data from the VLA, with resolution  $108.3'' \times 92.5''$ , centred on SS 433. The greyscale runs from 0 to  $2 \text{ Jy beam}^{-1}$ , and the rms noise in the image is  $192 \text{ mJy beam}^{-1}$ . The Galactic plane and several prominent sources are indicated.

older, optically thin material. A minimum energy calculation, using the 350-MHz flux density of the central source, gives a minimum energy of  $5 \times 10^{45}$  erg, which, combined with an estimate of the volume enclosed by the resolution element, gives a minimum power of order 25 per cent of the Eddington luminosity, consistent with the classification of the source as highly-accreting.

The image of the GRS 1915+105 field is shown in Figure 2. The majority of the bright sources are clustered around the Galactic Plane, and consist of H II regions and supernova remnants, notably G 46.8-0.3 (in the northeast corner of the 92-cm image), G 45.7-0.4 to the east of GRS 1915+105, and W 51 (the extended emission in the northeast corner of the 2-m image). GRS 1915+105 was detected at a level of  $21 \pm 6 \text{ mJy}$  in the 92-cm band, but not detected in the LFFE band. From simultaneous Ryle Telescope monitoring (G. Pooley, priv. comm.), its spectrum between 15 GHz and 350 MHz was steep, with a spectral index of  $-0.5 \pm 0.2$ . This suggests that at the lower frequency, we are seeing relic optically-thin emission from a flare, rather than the self-absorbed flat-spectrum plateau-state jet.

The field surrounding Cygnus X-3 is shown in Figure 3. At 2 m, the field is dominated by the non-thermal supernova remnant G 78.2+2.1. At 92 cm, the primary beam attenuates the emission from this source, and more nebulous, mainly thermal, emission is visible. This comprises com-

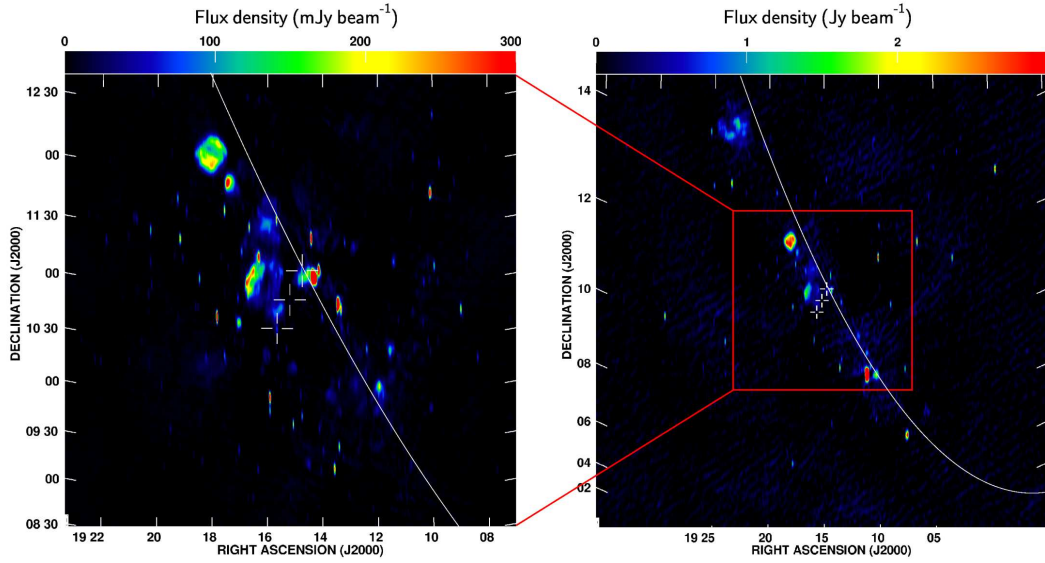


**Figure 2:** *Left:* 92-cm WSRT image of the field surrounding GRS1915+105. *Right:* LFFE 2-m image of the field surrounding GRS1915+105. The red box shows the 92-cm field. The central cross marks the position of GRS1915+105, and the two on either side are the proposed locations of the interactions of the jets with the interstellar medium [10]. White lines trace the Galactic plane.

plexes of H II regions, and optically-thin filaments interpreted as structures ionised by the strings of B stars that they contain [12]. Cygnus X-3 itself was not detected, to a  $3\sigma$  limit of 18 and 81 mJy in the 92-cm and LFFE 2-m bands respectively, which, taken together with the simultaneous 15-GHz monitoring at the Ryle Telescope [9] which measured a flux density of  $108 \pm 6$  mJy, suggests that the source spectrum between 350 MHz and 15 GHz was more inverted than  $\nu^{0.5}$ . Either the source is self-absorbed at the low frequencies, or free-free absorption along the line of sight to the source prevents us from detecting it. The companion is a Wolf-Rayet star with a strong stellar wind, and the line of sight passes through the Cygnus OB 2 association, making free-free absorption a plausible scenario.

### 3.2 The 2006 May outburst of Cygnus X-3

Cygnus X-3 underwent one of its giant outbursts beginning on 2006 May 4, which was tracked in a multiwavelength observing campaign, with e-VLBI imaging [11] showing a jet-like morphology. The source was detected in the LFFE 2-m band in all four of our observations, peaking at 2.3 Jy on 2006 May 20, before declining to 0.55 Jy by 2006 June 10. Figure 4 shows the measurements, together with the 15-GHz lightcurve from daily monitoring with the Ryle Telescope (G. Pooley, priv. comm.), and the derived spectral indices. The spectral index between 15 GHz and 140 MHz initially decreased (the spectrum steepened) as the lower-frequency emission became optically thin, after which re-flaring at 15 GHz, either due to further ejections or to shocks forming within the flow, caused the two-point spectrum to flatten once again. The peak flux density during the flare was a factor of 28 greater than the  $3\sigma$  upper limit from the observation of 2005 July, demonstrating that Cygnus X-3 is a highly variable object, even at frequencies as low as 140 MHz.

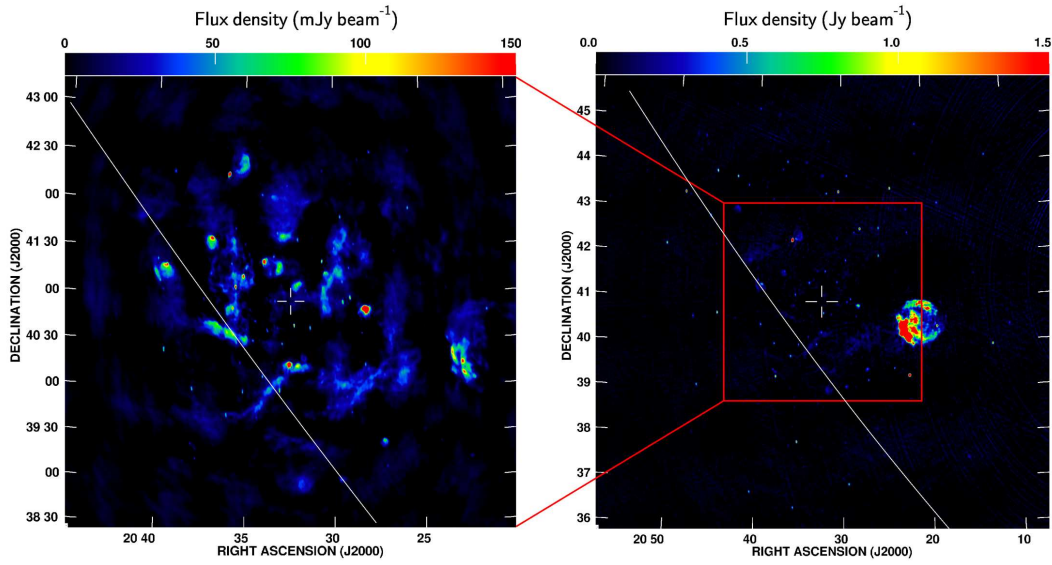


**Figure 3:** *Left:* 92-cm WSRT image of the field surrounding Cygnus X-3. *Right:* LFFE 2-m image of the field surrounding Cygnus X-3, whose position is marked with a cross. The red box shows the 92-cm field. White lines trace the Galactic plane.

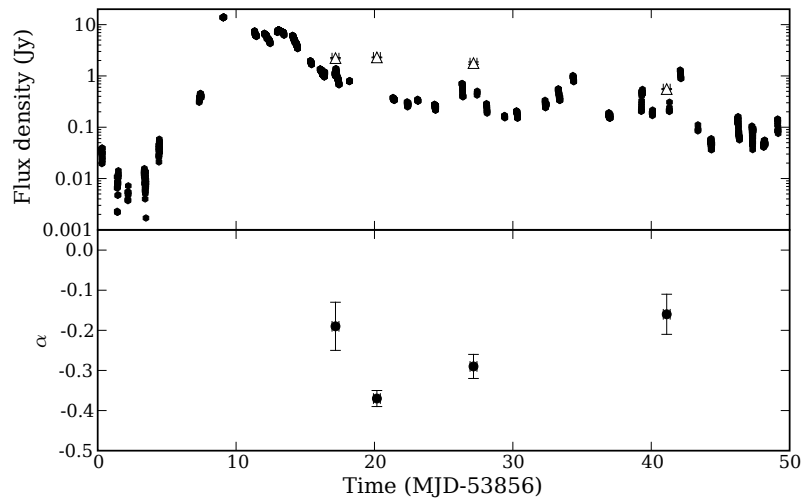


**Figure 4:** *Top:* 15-GHz lightcurve of the May 2006 outburst of Cygnus X-3 (black dots), with the open triangles representing the LFFE 2-m measurements. *Bottom:* Spectral index between 15 GHz and 140 MHz.

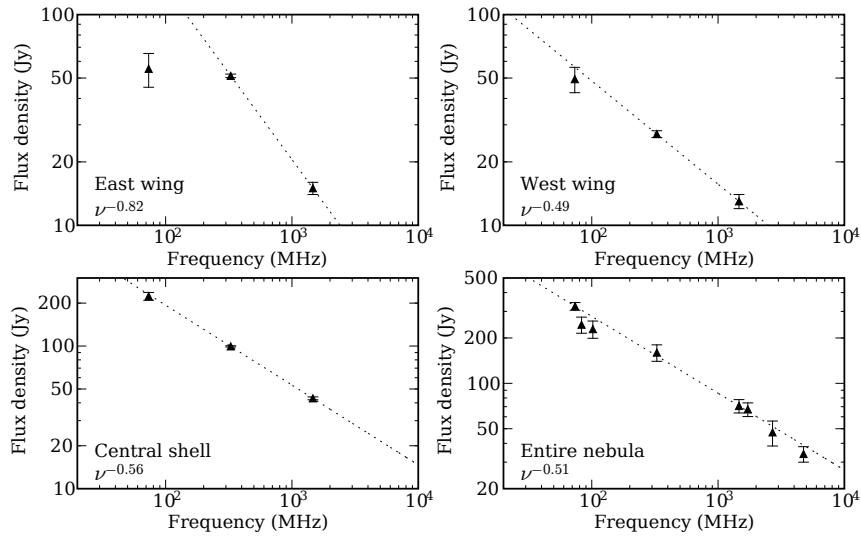


**Figure 5:** Spectra of the different components of the W50 nebula. *Top left:* Eastern wing. *Top right:* Western wing. *Bottom left:* Central shell. *Bottom right:* Entire nebula, including previous measurements [4, 8, 3]. Dashed lines show the spectral indices between 1465 and 327.5 MHz previously derived [4] for the components of the nebula, and in the bottom right plot, our derived spectrum of  $\alpha = -0.51 \pm 0.02$ .

### 3.3 Jet-blown bubbles

A subsidiary goal of the observations was to search for any evidence for the interaction of the jets of these systems on their surroundings. This is known to occur in SS 433, where the action of the precessing jets has deformed the surrounding W 50 nebula so that two wings protrude to the east and west of the quasi-circular nebula, in direct alignment with the axis of the jet precession cone [4]. From our observations, we were able to extend the known spectrum of W 50 down to 74 MHz, showing that it is an unbroken power law of spectral index  $-0.51$  without any evidence for a turnover except in the eastern wing (Figure 5). This suggests either additional low-frequency absorption along the line of sight to the eastern wing, or an underlying curved electron energy spectrum in this part of the nebula.

In GRS 1915+105, two IRAS sources either side of the central source (marked by crosses in Figure 2) have been proposed to be the sites of jet-ISM interactions [10]. We found no evidence for any link between these and the central source, nor for any lobes or bubbles inflated by the jets, consistent with the results of [1]. Neither did we find any evidence for extended emission associated with Cygnus X-3. This suggests that the external density and pressure in the environments of these two sources are insufficient to confine the jets [7].

## 4. Conclusions and Future Work

From these observations, it is clear that not all X-ray binaries are turned over at low radio frequencies, and that such objects are variable sources in the low-frequency sky. We confirm the highly-accreting nature of SS 433, and the extreme variability of Cygnus X-3 during outburst. The wide fields of view available at low frequencies make the concept of a radio all-sky monitor feasible

for the first time, and daily monitoring of the Galactic Plane with such an instrument will certainly detect variability. The upcoming generation of new low-frequency radio facilities, such as the Low Frequency Array (LOFAR), the Murchison Widefield Array (MWA) and the Long Wavelength Array (LWA) will detect sources such as these, making the prospects bright for detecting and studying transient events both within and outside the Galaxy.

These results are only preliminary, and more detailed analysis of these rich datasets can and will be carried out. With the multiple spectral windows available from the LFFEs, it will be possible to measure the spectrum of Cygnus X-3 between 117 and 175 MHz during its outburst, for comparison with the higher frequency RATAN and Ryle Telescope monitoring programmes. Further data on the weaker outburst of 2006 February is also available for similar analysis. With the multiple epochs, and such a wide field of view, the images may also be differenced to search for other variable sources in this densely-populated region of the Galaxy.

## 5. Acknowledgments

The National Radio Astronomy Observatory is a facility of the National Science Foundation operated under cooperative agreement by Associated Universities, Inc.

## References

- [1] S. Chaty, L. F. Rodríguez, I. F. Mirabel, T. R. Geballe, Y. Fuchs, A. Claret, C. J. Cesarsky, and D. Cesarsky, *A&A* **366**, 1035–1046 (2001).
- [2] W. D. Cotton, J. J. Condon, R. A. Perley, N. Kassim, J. Lazio, A. Cohen, W. Lane, and W. C. Erickson in proceedings of *Ground-based Telescopes. Edited by Oschmann, Jacobus M., Jr. Proceedings of the SPIE, Volume 5489, pp. 180-189 (2004).*, (J. M. Oschmann, Jr., ed.), Presented at the Society of Photo-Optical Instrumentation Engineers (SPIE) Conference, vol. 5489, October 2004, pp. 180–189.
- [3] A. J. B. Downes, C. J. Salter, and T. Pauls, *A&A* **103**, 277–287 (1981).
- [4] G. M. Dubner, M. Holdaway, W. M. Goss, and I. F. Mirabel, *AJ* **116**, 1842–1855 (1998).
- [5] R. P. Fender, R. A. M. J. Wijers, B. Stappers, R. Braun, M. Wise, T. Coenen, H. Falcke, J.-M. Griessmeier, M. Van Haarlem, P. G. Jonker, C. Law, S. Markoff, J. Masters, J. C. A. Miller-Jones, R. Osten, B. Scheers, H. Spreuw, J. Swinbank, C. Vogt, R. Wijnands, and P. Zarka, *The LOFAR Transients Key Project* in proceedings of *VI Microquasar Workshop: Microquasars and Beyond*, , 2006.
- [6] E. Gallo, R. Fender, C. Kaiser, D. Russell, R. Morganti, T. Oosterloo, and S. Heinz, *Nature* **436**, 819–821 (2005).
- [7] S. Heinz, *A&A* **388**, L40–L43 (2002).
- [8] A. V. Kovalenko, A. V. Pynzar', and V. A. Udal'Tsov, *AZh* **71**, 110–119 (1994).
- [9] G. G. Pooley and R. P. Fender, *MNRAS* **292**, 925–933 (1997).
- [10] L. F. Rodríguez and I. F. Mirabel, *A&A* **340**, L47–L50 (1998).
- [11] V. Tudose, R. P. Fender, M. A. Garrett, J. C. A. Miller-Jones, Z. Paragi, R. E. Spencer, G. G. Pooley, M. van der Klis, and A. Szomoru, *MNRAS* **375**, L11–L15 (2007).
- [12] H. J. Wendker, L. A. Higgs, and T. L. Landecker, *A&A* **241**, 551–580 (1991).